

1                               **Response to CO<sub>2</sub> doubling of**  
2                               **the Atlantic Hurricane Main Development Region**  
3                               **in a High-Resolution Climate Model**  
4  
5  
6

7       Takeshi Doi<sup>1,2</sup>, Gabriel A. Vecchi<sup>2</sup>, Anthony J. Rosati<sup>2</sup>, and Thomas L. Delworth<sup>2</sup>  
8  
9  
10

11    *1 Atmospheric and Oceanic Sciences Program, Princeton University, Princeton, NJ, U.S. A.*

12    *2 NOAA/Geophysical Fluid Dynamics Laboratory, Princeton, NJ, U.S.A.*  
13  
14  
15  
16

17                               Submitted to *Notes and Correspondence in J. Climate*  
18                               (Feb. 10, 2012)  
19  
20

21    

---

  
22    *Corresponding author address: Takeshi Doi, Geophysical Fluid Dynamics*  
23    *Laboratory/NOAA, Princeton University Forrestal Campus, 201 Forrestal Road, Princeton,*  
24    *NJ 08542, USA*  
25    *Tel: +1-609-452-6511*  
26    *Email: Takeshi.Doi@noaa.gov*

## Abstract

Response of climate conditions in the Atlantic Hurricane Main Development Region (MDR) to doubling of atmospheric CO<sub>2</sub> has been explored, using the new high-resolution coupled Climate Model version 2.5 developed at the Geophysical Fluid Dynamics Laboratory (GFDL-CM2.5). In the annual mean, the SST in the MDR warms by about 2°C in the CO<sub>2</sub> doubling run relative to the Control run, the trade winds become weaker in the northern tropical Atlantic, and the rainfall increases over the ITCZ and its northern region. The amplitude of the annual cycle of the SST over the MDR is not significantly changed by CO<sub>2</sub> doubling. However, we find that the interannual variations show significant responses to CO<sub>2</sub> doubling: the seasonal maximum peak of the interannual variations of the SST over the MDR moves from boreal spring to early boreal summer, at which time it is about 25% stronger than in the Control run. The enhancement of the interannual variations of the SST in the MDR is due to changes in effectiveness of the Wind-Evaporation-SST (WES) positive feedback: WES remains a positive feedback until boreal early summer in the CO<sub>2</sub> doubling run. This change in the interannual variability will be a factor in predicting the year-to-year risk of serious damages associated with the Atlantic Hurricane and drought (or flood) in the Sahel and South America in a future climate.

## 1. Introduction

Future climate response of the northern tropical Atlantic SST is a topic of substantial research, in part because of its potential impact on regional extreme events. Recent studies suggest that the Atlantic Hurricane activity may be modified in a future climate due in part to warmer SST anomalies in the northern tropical Atlantic, although there are uncertainties to the sign and magnitude of the change (Emanuel 2005; Swanson 2008; Vecchi et al. 2008; Knutson et al. 2010; Villanini et al. 2011). Also, climate changes in the northern tropical Atlantic SST influence rainfall over South America and the Sahel region through the meridional migration of the ITCZ and the West African Monsoon (Chiang et al. 2003; Kushnir et al. 2005; Hagos and Cook 2008; Biasutti and Sobel 2009). Held et al. (2005) suggested that an observed drying trend in the Sahel may be due to both increased aerosol loading and increased greenhouse gases, although there remains some uncertainty regarding the response of the Sahel rainfall to greenhouse gases (Cook et al 2008). Interestingly, impacts of Atlantic variations are not restricted to the Atlantic Basin and can reach far to the Indian Ocean, the global Northern Hemisphere, and global climate (Zhang and Delworth 2006; Lu et al. 2006; Zhang et al. 2007; Sutton and Hodson 2005; 2007; Kucharski et al. 2008; Ding et al. 2011). Recently, Kucharski et al. (2011) suggested that the Atlantic warming in the 20th century might have reduced the Pacific warming through modifications of the Walker circulation using regionally coupled models.

Most previous work has mainly focused on response of the annual mean of the northern tropical Atlantic SST to a future climate and relatively less attention has been paid to response of the interannual variations to radiative forcing changes. The interannual variations of the northern tropical Atlantic SST are strongly phase-locked to the annual cycle, which is referred to as “seasonal phase-locking”: the SST anomalies develop from early boreal winter, reach a maximum in boreal spring, and decay abruptly in boreal summer (Doi et al. 2010). Reasonable simulation of this seasonal dependence in a climate model is critical for seasonal prediction of the Tropical Atlantic Variability, which can influence prediction of the year-to-year variations of the Atlantic Hurricane and drought (or flood) in the Sahel and South America (e.g. Zhao et al. 2009; 2010; Vecchi et al. 2011; Chen and Lin 2012). Therefore, in this manuscript, we explore future climate response of the seasonal phase-locking of the interannual variations of the northern tropical Atlantic SST.

In order to assess response of climate changes, it is desirable to use a model that reproduces the characteristic of observed variability. Therefore, for this study, we used present-day Control and CO<sub>2</sub> doubling runs with a new high-resolution fully atmosphere-ocean coupled general circulation model described in Delworth et al (2012); Climate Model version 2.5 developed at the Geophysical Fluid Dynamics Laboratory (GFDL-CM2.5). This model shows high performance in simulating seasonal-interannual variations in the tropical Atlantic, in particular the seasonal phase-locking of the interannual variations of the

northern tropical Atlantic SST (Doi et al. 2012). A brief description of the high-resolution CM2.5 modeling system and the experiments analyzed here is given in section 2. Using outputs from these experiments, we explored response to CO<sub>2</sub> doubling of the SST over the Atlantic Hurricane Main Development Region (MDR: 80°-20°W, 10°-25°N), which is referred to as the SST<sub>MDR</sub>. The SST<sub>MDR</sub> is used as the local positive correlated climate predictor for the Atlantic Hurricane statistical-dynamical prediction model developed by Vecchi et al (2011) and Villarini et al. (2011), the other negative correlated predictor for the Atlantic Hurricane being SST averaged in global tropics. The SST<sub>MDR</sub> is thus an important quantity to represent realistically in models and predict its further evolution. Changes of the annual mean and the annual cycle of the SST<sub>MDR</sub> are discussed in sections 3a and b. Response of the interannual variations of the SST<sub>MDR</sub> is discussed in section 3c. The final section presents a summary and discussion of the results.

## **2. Model (GFDL-CM2.5)**

GFDL-CM2.5 (Delworth et al. 2012; Doi et al. 2012) is a new high-resolution model version that derives closely from GFDL-CM2.1 (Delworth et al. 2006, Gnanadesikan et al. 2006, Stouffer et al. 2006, and Wittenberg et al. 2006). The oceanic component of CM2.5 uses a 0.25° horizontal resolution of MOM4p1 in the tropics with the z\* vertical coordinate (Griffies 2010; Griffies et al. 2012), which varies from 28km near the

1 tropics to 8km in polar regions. It has a similar oceanic component to that of the CM2.4  
2 model of Farneti et al. (2010). It is coupled to a 50km horizontal resolution atmosphere  
3 model with 32 vertical levels on a cubed-sphere grid (Lin 2004; Putman and Lin 2007).  
4 This formulation avoids the numerical problem of the convergence of meridians at the  
5 poles and allows grid boxes of roughly equal area over the globe. No flux adjustments are  
6 employed. The ocean model does not contain a parameterization for mesoscale eddy  
7 mixing. The land model is LM3 (Shevliakova et al. 2009; Milly et al. *in preparation*),  
8 which represents snow and rain interception on vegetation, as well as water phase change in  
9 the soil and snow pack. CM2.5 is initialized and forced in similar fashion to CM2.1  
10 (Delworth et al. 2012; Delworth et al. 2006); the oceanic initial condition is taken from the  
11 end of one-year spin-up from observed climatological conditions at rest and the  
12 atmospheric initial condition is taken from the end of a simulation with prescribed SSTs.

13         We used monthly mean outputs from a 280 year simulation of CM2.5 with 1990  
14 radiative forcing as the Control run. The idealized climate change response run is  
15 conducted from the present-day Control integration. The CO<sub>2</sub> doubling ( $2 \times \text{CO}_2$ )  
16 experiment of GFDL-CM2.5 is performed for 140 years following the framework described  
17 in Delworth et al 2012; the model is forced with a 1% per year increase in atmospheric CO<sub>2</sub>  
18 concentration from year 101 of the 1990 Control simulation and reaches CO<sub>2</sub> doubling after  
19 70 years. After that, the CO<sub>2</sub> concentration is held fixed at twice its present-day Control  
20 value and the integration continues thereafter. In this paper, model year 1 is defined as a

1 year when the CO<sub>2</sub> doubling run starts.

### 3. Results

#### a. Annual mean

We begin by exploring time series of the SST<sub>MDR</sub> in model year 1-140 of the Control and the CO<sub>2</sub> doubling runs (Fig. 1). In this paper, we focus on the model outputs after CO<sub>2</sub> stabilization because we are interested in equilibrium response and assessment of changes in variability through the transient forcing phase is not straightforward. As indicated in Fig.1, we can discuss response of steady state to CO<sub>2</sub> doubling in years 91-140, when the annual mean SST<sub>MDR</sub> in the 2×CO<sub>2</sub> experiment warms by about 2°C relative to the Control run. We thus calculate monthly climatologies by averaging monthly mean output for years 91-140.

Figure 2 shows response to CO<sub>2</sub> doubling of the annual mean surface climate in the tropical Atlantic, along with the mean state of the Control run. The reader is referred to Doi et al (2012) for a discussion of the tropical Atlantic biases from observations in this model; CM2.5 successfully simulates seasonal-interannual variations of the northern tropical Atlantic SST and precipitation. The warming of SST in the Northern Hemisphere is about 0.2°C larger than that in the Southern Hemisphere (Fig. 2b). This meridional gradient

of the response to CO<sub>2</sub> doubling of SST has an associated northward migration of the Atlantic ITCZ (Fig. 2d), which results in southwesterly wind anomalies and thus weaker trade winds in 5°-20°N (Fig. 2f). We found 20% more rainfall over the ITCZ and its northern region, while 20% less rainfall over the southern region of the ITCZ and South America. The hemispheric asymmetric response of the annual mean SST, precipitation, and wind fields to CO<sub>2</sub> doubling in CM2.5 is consistent with the climate change response of the annual mean fields across other climate models shown in Xie et al. 2010. They showed that a greater warming in the Northern Hemisphere than in the Southern Hemisphere is accorded with asymmetries in trade wind changes. However, they focused on the annual mean fields changes and did not examine response of seasonal and interannual variations to CO<sub>2</sub> doubling, which will be shed light on in next subsections.

## **b. Mean seasonal cycle**

It is plausible to expect that the significant changes of the annual mean fields could connect to changes in the mean seasonal cycle. However, analysis of response of the seasonal variation of the surface climate in the MDR to CO<sub>2</sub> doubling does not indicate any substantial changes. For example, the difference of the amplitude of the seasonal cycle of the SST<sub>MDR</sub> between the Control run and the CO<sub>2</sub> doubling run is small and not significant, which is less than 5% of the amplitude of the seasonal cycle in the Control run (Fig. 3). We



1 note that the annual cycle of the  $SST_{MDR}$  is slightly delayed due to  $CO_2$  doubling. This is  
2 consistent with Biasutti and Sobel (2009), although that response is not significantly shown  
3 from monthly data.

4 Although significant changes in the seasonal cycle are not identified, it is possible  
5 that the magnitude and the seasonal phase-locking of the interannual variability may change  
6 in response to  $CO_2$  doubling. We explore this possibility in next subsection.

### 7 8 **c. Interannual variations**

9  
10 To assess interannual variability, we define anomaly fields as deviations from the  
11 monthly mean climatology. We remove the decadal variability using an eight-year running  
12 mean filter on a basis of spectrum analysis, because we focus on the interannual variation  
13 of the  $SST_{MDR}$  rather than its decadal variability.

14 Monthly standard deviations of the interannual anomalies of the  $SST_{MDR}$  are  
15 shown in Fig. 4. Interestingly, we find that the maximum peak in variability in the  $CO_2$   
16 doubling run appears in May, which is two months later than that in the Control run. The  
17 maximum difference in interannual variability between the  $CO_2$  doubling run and the  
18 Control run appears in June. The interannual variation of the  $SST_{MDR}$  in May-July is 25%  
19 stronger in the  $CO_2$  doubling run relative to the Control run. The separation of  $2 \times CO_2$   
20 response of the other 50-years mean standard deviations from the full years of the Control

run suggests that the enhancement of the interannual variations due to CO<sub>2</sub> doubling during early boreal summer is robust relative to the natural variability exhibited by the available Control run outputs, although the Control run varies to some extent. The natural variability of the interannual variations of the SST<sub>MDR</sub> in the Control run is also very interesting, but it is beyond the scope of this paper.

We explore a composite analysis to help understanding the mechanism of the response to CO<sub>2</sub> doubling of the interannual variations of the SST<sub>MDR</sub>. We construct a composite by averaging, based on selecting warm (cold) SST<sub>MDR</sub> years, when the SST<sub>MDR</sub> anomaly exceeds one standard deviation in month of the maximum peak. The details are shown in Table 1.

In the warm SST<sub>MDR</sub> year composite, the SST<sub>MDR</sub> anomaly in the Control run is 0.42°C in the maximum peak month of April, while the SST<sub>MDR</sub> anomaly in the CO<sub>2</sub> doubling run is 0.55°C in the maximum peak month of June. The maximum difference in the SST<sub>MDR</sub> anomaly between the Control run and the CO<sub>2</sub> doubling run is found in June, when the SST<sub>MDR</sub> anomaly warms by about 0.2°C in the CO<sub>2</sub> doubling run relative to the Control run (Fig. 5). The warm SST<sub>MDR</sub> anomaly in the CO<sub>2</sub> doubling run is significantly enhanced by 60% in June relative to the Control run. Interestingly, observations indicate that such an enhancement of interannual variability may be present in the historical record (Fig. 5a). The Hadley Center SST (HadISST; Rayner et al. 2003) shows that the interannual SST anomaly in warm SST<sub>MDR</sub> years is warmer by about 0.15°C in a warmer climate of the

recent 50 years (1960-2009) relative to the early 50 years (1881-1930), although the extent to which this observed change is due to radiative forcing or internal variability remains to be determined.

To explore the mechanism behind the change in interannual variability, we calculated the diagnostic bulk mixed-layer heat budget over the MDR;

$$\frac{\partial T_{mix}}{\partial t} = \frac{Q - q_{sw}}{\rho C_p H_{mix}} + \text{ocean dynamics contribution} . \quad (1)$$

Here,  $T_{mix}$  is the mixed-layer temperature, a proxy for SST,  $\rho$  is the typical sea water density ( $1025 \text{ kg m}^{-3}$ ),  $C_p$  is the typical heat capacity of the sea water ( $3996 \text{ J kg}^{-1} \text{ K}^{-1}$ ), and  $H_{mix}$  is the mixed-layer depth, which is calculated monthly as the depth at which the potential density becomes  $0.125 \text{ kg m}^{-3}$  larger than the surface density, as used by Levitus (1982). The quantity  $Q$  denotes the net surface enthalpy flux (including shortwave radiation, longwave radiation, latent heat flux, and sensible heat flux), and  $q_{sw}$  is the downward solar insolation that penetrates below the bottom of the mixed-layer. Thus, the first term on the right hand side,  $\frac{Q - q_{sw}}{\rho C_p H_{mix}}$ , represents the influence of atmospheric thermal forcing on the mixed-layer heat budget, which is referred as “the surface enthalpy flux contribution” hereafter. Note that “the surface enthalpy flux contribution” is different from  $Q$ : “the net surface enthalpy flux”. The ocean dynamical contribution is simply estimated by difference between rate of change of the mixed-layer temperature and the surface enthalpy flux contribution.

In the Control run, the warming tendency of the SST<sub>MDR</sub> during boreal spring is mainly due to the surface enthalpy flux contribution until April, when the warm SST<sub>MDR</sub> starts to decay (Fig. 6a). Meanwhile, in the CO<sub>2</sub> doubling run, the warm SST<sub>MDR</sub> anomalies still keep warming until June (Figs. 6b). The maximum difference of the warming tendency between the Control run and the CO<sub>2</sub> doubling run is found in May, arising mainly from differences in the surface enthalpy flux contribution (Fig. 6c). We note that interannual variations of surface enthalpy flux contribution,  $\frac{Q - q_{sw}}{\rho C_p H_{mix}}$  in Eq. 1, includes not only interannual variations of surface enthalpy flux, but also interannual variations of mixed-layer depth. However, we have confirmed that interannual variations of mixed-layer depth do not contribute to the differences in the surface enthalpy flux contribution over the MDR in boreal spring-summer (figure not shown).

The surface enthalpy flux anomalies, i.e. the  $Q$  anomalies, from boreal winter through boreal spring are dominated by wind-induced latent heat flux anomalies in the Control run and the CO<sub>2</sub> doubling run (Figs. 6d and e). It suggests that the Wind-Evaporation SST (WES) positive feedback (Xie 1999) develops the warm SST anomalies over the northern tropical Atlantic similarly both in the Control run and the CO<sub>2</sub> doubling run; the WES positive feedback is associated with the meridional migration of the ITCZ: 1) an anomalously northward migration of the ITCZ causes southwesterly wind anomalies in the northern tropics leading to weaker trade winds, 2) this results in less evaporation and thus suppressed latent heat loss from ocean, leading to warmer SST in the northern tropical

Atlantic. 3) The outcome is the further northward migration of the ITCZ. The dominance of this mechanism in the growth of anomalies has been discussed in previous work (Carton et al. 1996; Chang et al. 1997; Xie 1999). Also, Doi et al. 2012 show that the WES feedback is reasonably captured in the Control run of CM2.5.

The principal difference in the surface enthalpy flux anomalies between the Control run and the CO<sub>2</sub> doubling run is found in May, which is due to latent heat flux, primarily the wind-induced component (Figs. 6c and f). We also note the shortwave contribution in May, although it does not show principal difference between the Control run and the CO<sub>2</sub> doubling run. In the Control run, both latent heat and shortwave radiative flux anomalies are important for driving the cooling tendency in May (Fig. 6d). The shortwave cooling arises mainly from increased cloud amount tied to the enhanced convection that follows the warm SST anomalies. In the CO<sub>2</sub> doubling run, the shortwave radiation anomalies are very similar to those in the Control run.

The difference in wind-induced latent heat flux anomalies between the Control run and the CO<sub>2</sub> doubling run can be written as  $(\frac{\partial Q_{LH}}{\partial W}\bigg|_{CO_2} W'_{CO_2} - \frac{\partial Q_{LH}}{\partial W}\bigg|_{CTL} W'_{CTL})$ , where  $Q_{LH}$  is latent heat flux,  $W'_{CO_2}$  and  $W'_{CTL}$  is the composite anomaly of the surface wind speed in the CO<sub>2</sub> doubling run and the Control run respectively. Figure 7 shows the difference in wind-induced latent heat flux anomalies and wind stress anomalies during April-June between the CO<sub>2</sub> doubling run and the Control run. It is suggested that the positive WES feedback has already ended in the Control run by April, while the WES feedback keeps

1 warming  $SST_{MDR}$  through June in the  $CO_2$  doubling run (Figs. 6d,e,f). In May, the weak  
2 anomalies of the trade winds are larger in the  $CO_2$  doubling run than those in the Control  
3 run (Fig. 7b), which enhance the suppressing of latent heat loss from ocean in the  $CO_2$   
4 doubling run (Fig. 7a).

5 We assume liner relation between the interannual anomalies of wind speed and  
6 those of SST over the MDR ( $W' \approx \alpha SST'$ ) (e.g. Maloney and Chelton 2006) and calculated  
7 the least squares estimate of the slope of this liner relation in model years 91-140. The  
8 slope in the  $CO_2$  doubling run in boreal spring is  $-0.80 \text{ m s}^{-1} \text{ per } ^\circ\text{C}$ , which is similar to -  
9  $0.83 \text{ m s}^{-1} \text{ per } ^\circ\text{C}$  in the Control run. However, in boreal summer, the slope in the  $CO_2$   
10 doubling run is  $-0.37 \text{ m s}^{-1} \text{ per } ^\circ\text{C}$ , which is about twice of  $-0.17 \text{ m s}^{-1} \text{ per } ^\circ\text{C}$  in the Control  
11 run. It shows that the coupling between the SST variations and the wind speed variations is  
12 stronger in the  $CO_2$  doubling run in boreal summer relative to the Control run.

13 Finally in this section, we estimate likely impacts on the Atlantic Hurricane  
14 activity and the rainfall field by the change in the characteristic of the interannual  
15 variability over the MDR. Table 2 gives Atlantic Hurricane counts estimated by the Atlantic  
16 Hurricane statistical-dynamical prediction model developed by Vecchi et al (2011), using  
17 the methodology of Villarini et al. (2011; 2012). Mean Atlantic Hurricane count decrease  
18 by 10% in the  $CO_2$  doubling run relative to the Control run. In warm (cold)  $SST_{MDR}$  year  
19 composite, the Atlantic Hurricane count increases (decreases) in observation, which is also  
20 consistent with Kossin and Vimont (2007). The Control run shows that the Atlantic

Hurricane count significantly increases by about 30% in warm SST<sub>MDR</sub> year relative to the mean count, while the CO<sub>2</sub> doubling run shows that the Hurricane count significantly increases in warm SST<sub>MDR</sub> year by about 45% relative to the mean count. Interestingly, the interannual increase of Hurricane count in warm SST<sub>MDR</sub> years is enhanced by 20% in the CO<sub>2</sub> doubling run relative to the Control run, even though the mean count shows reduction in the CO<sub>2</sub> doubling run. This large interannual variation of Atlantic Hurricane count is consistent with the large interannual variability of the SST<sub>MDR</sub> in boreal early summer in the CO<sub>2</sub> doubling run. Also, the warm SST<sub>MDR</sub> anomalies in boreal early summer in the CO<sub>2</sub> doubling run are associated with the northward migration of the ITCZ: more rainfall over 5°-10°N and less rainfall over 5°N-5°S and South America (Fig. 5c). Note that the cold SST<sub>MDR</sub> years can be explained by using similar mechanisms of opposite sign to the warm years (figures not shown). As shown in Table 2d, the interannual decrease of Hurricane count in cold SST<sub>MDR</sub> years is enhanced by 33% in the CO<sub>2</sub> doubling run relative to the Control run.

#### **4. Summary and discussions**

Using outputs from present-day Control and CO<sub>2</sub> doubling runs with the new high-resolution fully coupled GCM (GFDL-CM2.5), response of SST over the Atlantic hurricane Main Development Region (SST<sub>MDR</sub>) to CO<sub>2</sub> doubling has been investigated. The

1 annual mean SST<sub>MDR</sub> increases by about 2°C in the CO<sub>2</sub> doubling run relative to the Control  
2 run and by about 0.3°C more than the southern tropical Atlantic. The warmer SST<sub>MDR</sub> drives  
3 a northward migration of the Atlantic ITCZ, which causes southwesterly wind anomalies  
4 and thus weaker trade winds in the northern tropical Atlantic. The SST, wind, and  
5 precipitation changes seem to develop in a positive WES feedback. This is consistent with  
6 Xie et al. (2011), who discussed that latent heat flux are important for the climate change  
7 pattern of the annual mean SST via the WES feedback.

8         The amplitude of the annual cycle of the SST<sub>MDR</sub> is not significantly changed due  
9 to CO<sub>2</sub> doubling. However, we find a significant change of the interannual variations: the  
10 maximum peak of the interannual variations of the SST<sub>MDR</sub> in the CO<sub>2</sub> doubling run moves  
11 from boreal spring to early boreal summer, at which time it is about 25% stronger relative  
12 to the Control run. The enhancement of the interannual variation of SST<sub>MDR</sub> in boreal early  
13 summer also seems to appear in the observation, although there are some uncertainties  
14 among observational datasets. The large interannual variations of the SST<sub>MDR</sub> during early  
15 boreal summer in the CO<sub>2</sub> doubling run is due to changes in the effectiveness of the WES  
16 positive feedback in a warmer climate: WES remains a positive feedback until early boreal  
17 summer in the CO<sub>2</sub> doubling run.

18         The large amplitude of the interannual variation of the SST<sub>MDR</sub> in boreal early  
19 summer due to CO<sub>2</sub> doubling could be a factor of severe damage of the enhanced year-to-  
20 year variations of Atlantic Hurricanes (Table 2) and drought (or flood) in the South



American and Sahel region (Fig. 5c). Therefore, we should pay more attention to this enhancement of the interannual variability of the SST<sub>MDR</sub> in a warmer climate, although most previous work has mainly focused on the future climate change of the annual mean SST and relatively less attention has been paid to response of the interannual variations.

The ultimate cause for the response to CO<sub>2</sub> doubling of the interannual modulation of the meridional migration of the ITCZ and the WES feedback is still open to debate. We showed that the effectiveness of the WES feedback in early boreal summer is stronger in the CO<sub>2</sub> doubling run relative to the Control run. The difference in wind speed anomalies between the CO<sub>2</sub> doubling and the Control run is important for the interannual SST variations in the northern tropical Atlantic. Also, the coupling between the SST variations and the wind speed variations is stronger in the CO<sub>2</sub> doubling run during boreal summer. The long-lasting interannual WES feedback in a warmer climate may be related to the annual mean changes. The response of the annual mean SST, wind, and precipitation to CO<sub>2</sub> doubling seems to be coupled via a positive WES feedback. The characteristic of the enhancement of a positive WES feedback in the annual mean may lead to the large year-to-year variations around the annual mean. Also, the difference in the wind anomalies over the MDR between the CO<sub>2</sub> doubling and the Control run seems to be significantly related to the zonal wind in the eastern Pacific in 5°-10°N (figure not shown). Previous work showed that strong ENSO events in the Pacific can partly lead to the warm SST in the northern tropical Atlantic (see Xie and Carton 2004 for a recent review on the Tropical Atlantic Variability).

Results from GFDL-CM2.1 and CM2.5 suggest that the amplitude of ENSO events is slightly stronger in the CO<sub>2</sub> doubling experiment than in the Control run (A. Wittenberg, pers. comm.; Delworth et al. 2012). Also, Czaja (2004) suggested that the seasonal dependence of the interannual variability in the northern tropical Atlantic is reflected not only by Atlantic local air-sea coupling, but also by the remote forcing of the North Atlantic Oscillation and ENSO. Biasutti and Sobel (2009) discussed the idea that the delayed phase of the West African monsoon in a warmer climate is due to sea ice loss at high-latitudes. For the Atlantic Hurricane prediction, not only SST<sub>MDR</sub>, but also the global tropical mean SST is important (Zhao et al. 2009; Zhao et al. 2010; Vecchi et al. 2011). Exploring the relation between the Northern Tropical Atlantic and other basins will be the focus of further work.

Finally, we discuss robustness of our main new result: the enhancement of the interannual variation of SST<sub>MDR</sub> in boreal early summer due to CO<sub>2</sub> doubling. Breugem et al. (2007) show that the Atlantic Meridional Mode weakens in the CO<sub>2</sub> doubling run with an atmospheric model coupled to a mixed-layer ocean model. It may be difficult to realistically identify the robust response of the Tropical Atlantic Variability to CO<sub>2</sub> doubling in coupled GCMs, since almost all CMIP3 climate models had serious biases in the annual mean tropical Atlantic (Richter and Xie 2008) and the seasonal phase-locking of the interannual variations of the northern tropical Atlantic SST (figure not shown). However, the climatology of tropical North Atlantic variability in the high-resolution coupled model

used here is substantially improved relative to previous generation models (Doi et al. 2012). Further intercomparisons among coupled climate models with reduced tropical Atlantic biases will help clarifying the robustness of our results, which have new important implications and make solid progress for tropical Atlantic climate.

## **Acknowledgments**

We thank to Drs. Andrew Wittenberg, Ming Zhao, Rym Msadek, and Ian Lloyd for helpful comments and suggestions. We are grateful to the GFDL-CM2.5 modeling team for their assistance with model infrastructure support and data processing.

## References

- Biasutti, M., and A. H. Sobel, 2009: Delayed Sahel rainfall and global seasonal cycle in a warmer climate. *Geophys. Res. Lett.*, **36**, L23707, doi:10.1029/2009GL041303.
- Breugem, W.-P., W. Hazeleger, and R. J. Haarsma, 2007: Mechanism of Northern Tropical Atlantic Variability and response to CO<sub>2</sub> doubling. *J Climate*, **20**, 2691-2705.
- Carton, J. A., X. Cao, B. S. Giese, and A. M. da Silva, 1996: Decadal and interannual SST variability in the tropical Atlantic Ocean. *J. Phys. Oceanogr.*, **26**, 1165-1175.
- Chang, P., L. Ji, and H. Li, 1997: A decadal climate variation in the tropical Atlantic ocean from thermodynamic air-sea interactions. *Nature*, **385**, 516-518.
- Chen, J. H., and Shian-Jiann Lin, 2012: The remarkable predictability of inter-annual variability of Atlantic hurricanes during the past decade. *Geophys. Res. Lett.*, **38**, L11804, DOI:10.1029/2011GL047629.
- Chiang, J. C. H., M. Biasutti, and D. S. Battisti, 2003: Sensitivity of the Atlantic ITCZ to Last Glacial Maximum boundary conditions. *Paleoceanography*, **18**, doi:10.1029/2003PA000916.
- Cook, K., 2008: The mysteries of Sahel droughts. *Nature Geoscience*, **1**, 647-648.
- Czaja, A., 2004: Why is North Tropical Atlantic SST variability stronger in boreal spring? *J. Climate*, **17**, 3017-3025.
- Delworth, T. L., and Coauthors, 2006: GFDLs CM2 global coupled climate models. Part

I : Formulation and simulation characteristics. *J. Climate*, **19**, 643-674.

Delworth, T. L., and Coauthors, 2012: Simulated climate and climate change in the GFDL-CM2.5 high-resolution coupled climate model. *J. Climate*, *in press*

Ding, H., N. S. Keenlyside, M. Latif, 2011: Impact of the equatorial Atlantic on the El Niño Southern Oscillation. *Climate Dyn.*, DOI: 10.1007/s00382-011-1097-y.

Doi, T., G. A. Vecchi, A. J. Rosati, and T. L. Delworth, 2012: Tropical Atlantic biases in the mean state, seasonal cycle, and interannual variations for a coarse and a high resolution coupled climate model, submitted to *J. Climate*.

Emanuel, K., 2005: Increasing destructiveness of tropical cyclones over the past 30 years. *Nature*, **436**, 686-688.

Farneti, R., T. L. Delworth, A. J. Rosati, S. M. Griffies, F. Zeng, 2010: The role of mesoscale eddies in the rectification of the Southern Ocean response to climate change. *J. Phys. Oceanogr.*, **40**, 1539–1557.

Gnanadesikan, A., and Coauthors, 2006: GFDL's CM2 global coupled climate models. Part II: The baseline ocean simulation. *J. Climate*, **19**, 675–697.

Griffies, S. M., 2010: Elements of MOM4p1. *GFDL OCEAN GROUP TECHNICAL REPORT NO. 6*, p444.

Griffies, S. M., and coauthors, 2012: GFDL's CM3 Coupled climate model: characteristics of the ocean and sea ice simulations. *Journal of Climate*, *in press*.

Hagos, S. M., and K. H. Cook, 2009: Development of a coupled regional model and its

1 application to the study of interactions between the West African monsoon and the  
2 eastern tropical Atlantic Ocean. *J. Climate*, **22**, 2591-2604.

3 Held, I. M., T. L. Delworth, J. Lu, K. L. Findell, and T. R. Knutson, 2005: Simulation of  
4 Sahel drought in the 20th and 21st centuries. *Proc. Natl. Acad. Sci.*, **102**, 17891–17896.

5 Knutson, T. R., coauthors, 2010: Tropical cyclones and climate change. *Nature Geoscience*  
6 **3**, 157-163.

7 Kossin, J. P., and D. J. Vimont, 2007: A more general framework for understanding Atlantic  
8 hurricane variability and trends. *Bull. Amer. Meteor. Soc.*, **88**, 1767–1781.

9 Kucharski, F., A. Bracco, J. Y. Yoo, and F. Molteni, 2008: Atlantic forced component of the  
10 Indian monsoon interannual variability. *Geophys. Res. Lett.*, **35**,  
11 doi:10.1029/2007GL033037.

12 Kucharski, F., I.-S. Kang, R. Farneti, and L. Feudale, 2011: Tropical Pacific response to  
13 20th century Atlantic warming, *Geophys. Res. Lett.*, **38**, doi:10.1029/2010GL046248.

14 Kushnir, Y., W. A. Robinson, P. Chang, and A. W. Robertson, 2006: The physical basis for  
15 predicting Atlantic sector seasonal to interannual climate variability. *J. Climate*, **19**,  
16 5949-5970.

17 Levitus, S., 1982: Climatological Atlas of the World Ocean, NOAA Professional Paper 13,  
18 U.S. Department of Commerce.

19 Lin, S.-J., 2004: A “vertically Lagrangian” finite-volume dynamical core for global models.  
20 *Mon. Wea. Rev.*, **132**, 2293-2307.

- 1 Lu, R., B. Dong, and H. Ding (2006), Impact of the Atlantic Multidecadal Oscillation on  
2 the Asian summer monsoon, *Geophys. Res. Lett.*, **33**, doi:10.1029/2006GL027655.
- 3 Maloney, E. D., and D. B. Chelton, 2006: An assessment of the sea surface temperature  
4 influence on surface wind stress in numerical weather prediction and climate models. *J.*  
5 *Climate*, **19**, 2743-2762.
- 6 Meehl, G. A., and coauthors, 2007: The WCRP CMIP3 multimodel dataset - A new era in  
7 climate change research. *Bull. Amer. Meteor. Soc.*, **88**, 1383-1394.
- 8 Milly, P. C. D., S. L. Malyshev, E. Shevliakova, K. A. Dunne, K. L. Findell, K. Eng, T.  
9 Gleeson, Z. Liang, P. Phillips, R. J. Stouffer, and S. Swenson. Enhanced Representation  
10 of Land Physics for Earth-System Modeling. *in preparation*.
- 11 Putman, W M., and Shian-Jiann Lin, 2007: Finite-volume transport on various cubed-  
12 sphere grids. *J. Computational Phys.*, **227**, 55-78.
- 13 Rayner, N. A., and Coauthors, 2003: Global analyses of sea surface temperature, sea ice,  
14 and night marine air temperature since the late nineteenth century. *J. Geophys. Res.*, **108**,  
15 doi:10.1029/2002JD002670.
- 16 Richter, I., and S. P. Xie, 2008: On the origin of equatorial Atlantic biases in coupled  
17 general circulation models. *Climate Dyn.*, **31**, 587-598.
- 18 Shevliakova E, Pacala S, Malyshev S, Hurtt G, Milly P, Caspersen J, Sentman L, Fisk J,  
19 Wirth C, Crevoisier C. 2009. Carbon cycling under 300 years of land use change:  
20 Importance of the secondary vegetation sink. *Global Biogeochemical Cycles* **23**,

doi:10.1029/2007GB003176.

Smith, T. M., R. W. Reynolds, T. C. Peterson, J. Lawrimore, 2008: Improvements to NOAA's Historical Merged Land–Ocean Surface Temperature Analysis (1880–2006). *J. Climate*, **21**, 2283–2296.

Stouffer R. J., and Coauthors, 2006: GFDL's CM2 global coupled climate models. Part IV: Idealized climate response. *J. Climate*, **19**, 723–740.

Swanson K. L., 2008: Nonlocality of Atlantic tropical cyclone intensities. *Geochem. Geophys. Geosys.* **9**, Q04V01, doi:10.1029/2007GC001844.

Stouffer R. J., and Coauthors, 2006: GFDL's CM2 global coupled climate models. Part IV: Idealized climate response. *J. Climate*, **19**, 723–740.

Sutton R. T., and D. L. R. Hodson, 2005: Atlantic Ocean forcing of North American and European summer climate. *Science*, **309**, 115–118.

Sutton R. T., and D. L. R. Hodson, 2007: Climate response to basin-scale warming and cooling of the North Atlantic Ocean. *J. Climate*, **20**, 891–907.

Vecchi, G. A., K. L. Swanson, B. Soden, 2008: Whither hurricane activity? *Science*, **322**, 687–688,

Vecchi, G. A., M. Zhao, G. Villarini, A. Rosati, I. Held, and R. Gudgel, 2011: Hybrid statistical-dynamical predictions of seasonal Atlantic hurricane activity. *Mon. Wea. Rev.*, **139**, 1070–1082.

Villarini, G., G. A. Vecchi, T. R. Knutson, and J. A. Smith, 2011: Is the recorded increase in



1 short\_duration North Atlantic tropical storms spurious?, *J. Geophys. Res.*, **116**,

2 doi:10.1029/2010JD015493.

3 Villarini, G., G. A. Vecchi, and J. A. Smith, 2012: U.S. Landfalling and North Atlantic

4 Hurricanes: Statistical modeling of their frequencies and ratios, *Mon. Wea. Rev.*,

5 doi:10.1175/MWR-D-11-00063.1

6 Wittenberg, A. T., A. Rosati, N.-C. Lau, and J. J. Ploshay, 2006: GFDL's CM2 global coupled

7 climate models, Part 3: Tropical Pacific climate and ENSO. *J. Climate*, **19**, 698-722.

8 Xie, S. P., 1999: A dynamic ocean-atmosphere model of the tropical Atlantic decadal

9 variability. *J. Climate*, **12**, 64-70.

10 Xie, S. P., and J. A. Carton, 2004: Tropical Atlantic variability: patterns, mechanisms, and

11 impacts. *Earth's Climate: The Ocean-Atmosphere Interaction: From Basin to Global*

12 *Scales, Geophys. Monogr., Vol. 147, Amer. Geophys. Union*, 121-142.

13 Xie, S. P., C. Deser, G. A. Vecchi, J. Ma, H. Teng, and A. T. Wittenberg, 2011: Global

14 Warming pattern formation: sea surface temperature and rainfall. *J. Climate*, **23**, 966-

15 986.

16 Zhang, R., and T. L. Delworth, 2006: Impact of Atlantic multidecadal oscillations on

17 India/Sahel rainfall and Atlantic hurricanes. *Geophys. Res. Lett.*, **33**,

18 doi:10.1029/2006GL026267.

19 Zhao, M., I.M. Held, S.-J. Lin, and G. A. Vecchi, 2009: Simulations of global hurricane

20 climatology, interannual variability, and response to global warming using a 50km

- 1        resolutions GCM. *J. Climate*, **22**, 6653-6678.
- 2    Zhao, M, I.M. Held, and G. A. Vecchi, 2010: Retrospective forecasts of the hurricane
- 3        season using a global atmospheric model assuming persistence of SST anomalies. *Mon.*
- 4        *Wea. Rev.*, **138**, 3858-3868.

# Table1

**Table 1:** Summary for the interannual variations of the  $SST_{MDR}$  in CM2.5 for model years 91-140. (a) The peak month is defined as the maximum of the interannual variations of the  $SST_{MDR}$ . (b) The standard deviation of the interannual variations of the  $SST_{MDR}$  in the peak month ( $^{\circ}C$ ). (c) The number of warm  $SST_{MDR}$  years used for the composite analysis defined in the text.

	Control run	CO <sub>2</sub> doubling run
(a) Peak month	March	May
(b) Std. in peak month	0.29	0.32
(c) Num. of warm years	7 years	6 years

1 **Table 2:** Summary for Atlantic Hurricane count estimated by Hybrid Statistical-Dynamical  
2 Predictions Model of Villarini et al (2011) in model years 91-140. For comparison, we  
3 include observational estimates from the HadISST dataset in 1982-2005. (a) Annual mean  
4 Atlantic Hurricane count, which is calculated by averaging interannual estimates of  
5 Hurricane count. (b) Same as (a), but mean count is calculated by substitute mean SST  
6 difference to the model of Villarini et al (2011). The difference between (a) and (b) arises  
7 from the non-linearity of the model of Villarini et al (2011). Note that the characteristic of  
8 (a) and (b) is very similar. (c) Atlantic Hurricane count anomaly averaged in warm SST<sub>MDR</sub>  
9 years. Increasing (decreasing) is shown by positive (negative) value. A bold text shows a  
10 value beyond 90% significance level. Note that the interannual variations of Atlantic  
11 Hurricane count increases by about 20% in the CO<sub>2</sub> doubling run even the mean count  
12 shows reduction. (d) Same as (c), but for cold SST<sub>MDR</sub> years.

	(a) Mean $\frac{\sum_{y=91}^{y=140} f(y)}{50}$	(b) Mean $f(\overline{SST})$	(c) Warm SST <sub>MDR</sub> years	(d) Cold SST <sub>MDR</sub> years
Observation	6.51	6.36	+0.95	<b>-1.28</b>
CM2.5-Control	6.56	6.36	<b>+2.12</b>	<b>-1.07</b>
CM2.5-CO <sub>2</sub> doubling	5.88	5.69	<b>+2.55</b>	<b>-1.42</b>
CO <sub>2</sub> doubling run minus Control run	-0.68	-0.67	+0.43 (+20%)	-0.35 (-33%)

## Figure captions

Fig. 1: (a) SST averaged in the Main Developing Region for Atlantic Hurricane (MDR: 80°-20°W, 10°-25°N) from the present-day Control run (blue line) and its CO<sub>2</sub> doubling run (red line) with CM2.5 in model years 1-140 (°C). This paper focuses on model years 91-140. A running mean of eight years is applied.

Fig. 2: (a) Annual mean SST in the Control run averaged in model years 91-140 (°C). (b) Response to CO<sub>2</sub> doubling of annual mean SST (CO<sub>2</sub> doubling run minus Control run) in model years 91-140 (°C). Note that the change in annual mean SST between CO<sub>2</sub> doubling run and Control run is beyond one standard deviation of interannual variations of annual mean SST in the Control run everywhere in this figure. (c) Same as (a), but for rainfall (mm day<sup>-1</sup>). Contour interval is 1mm day<sup>-1</sup>. Red dashed line shows the latitude of the mean Atlantic ITCZ in the Control run. Grey shading denotes that the change in annual mean rainfall between CO<sub>2</sub> doubling run and Control run is beyond one standard deviation of interannual variations of annual mean rainfall in the Control run. (d) Same as (b), but for rainfall. Contour interval is 0.5mm day<sup>-1</sup>. (e) Same as (a), but for wind stress (N m<sup>-2</sup>). (f) Same as (b), but for wind stress (N m<sup>-2</sup>). Contour interval is 0.0025N m<sup>-2</sup>.

Fig. 3: Mean seasonal variations of SST<sub>MDR</sub> from the annual mean in the present-day Control (blue line) and the CO<sub>2</sub> doubling run (red line) (°C).

Fig. 4: (a) Monthly standard deviation of the interannual variation of the SST<sub>MDR</sub> for the present-day Control (thick blue line) and the CO<sub>2</sub> doubling run (thick red line) in model years 91-140 (°C). The thin blue lines show the four other 50-years mean standard deviations in the Control run. A running mean of three months is applied.

Fig.5: (a) Difference in composite anomalies for SST between the recent 50 years (1960-2009) minus the early 50 years (1881-1930) from the HadISST data for May-July in warm SST<sub>MDR</sub> years (°C). Contour interval is 0.1°C. Grey shading denotes anomalies above 90%

significance level. MDR is shown by solid box. (b) Similar to (a), but response to CO<sub>2</sub> doubling of composite anomalies for SST in the CO<sub>2</sub> doubling run minus the Control run. (c) Same as (b), but for rainfall in the CO<sub>2</sub> doubling run minus the Control run (mm day<sup>-1</sup>). Contour interval is 1mm day<sup>-1</sup>.

Fig. 6: Diagnostic bulk mixed-layer heat balance anomaly over the MDR (10<sup>-7</sup> K s<sup>-1</sup>). Rate of change of SST<sub>MDR</sub> is determined by  $\frac{Q - q_{sw}}{\rho C_p H_{mix}}$ : sea surface enthalpy flux contribution and ocean dynamical contribution by Eq. (1) in the text. A running mean of three months is applied. (a) Warm SST<sub>MDR</sub> years composite in the Control run of CM2.5. (b) Same as (a), but for the CO<sub>2</sub> doubling run. (c) Same as (a), but for difference between the CO<sub>2</sub> doubling run and the Control run. (d) Warm SST<sub>MDR</sub> years composite in the Control run for surface enthalpy flux anomaly over the MDR (W m<sup>-2</sup>).  $Q$ : net surface enthalpy flux anomaly “Net. Hflx” is determined by shortwave radiation “SW”, wind-induced latent heat “LH(wind)”, moisture-induced latent heat “LH(moisture)”, longwave radiation ‘LW’, and sensible heat “SH” fluxes. A running mean of three months is applied. (e) Same as (d), but for the CO<sub>2</sub> doubling run. (f) Same as (d), but for difference between the CO<sub>2</sub> doubling run and the Control run.

Fig. 7: (a) Response to CO<sub>2</sub> doubling of composite anomalies for the wind-induced latent heat flux in the CO<sub>2</sub> doubling run minus the Control run,  $\left. \frac{\partial Q_{LH}}{\partial W} \right|_{CO_2} W'_{CO_2} - \left. \frac{\partial Q_{LH}}{\partial W} \right|_{CTL} W'_{CTL}$  in the text, for April-June in warm SST<sub>MDR</sub> years (W m<sup>-2</sup>). Positive values shows warming ocean. Contour interval is 5W m<sup>-2</sup>. Color shading denotes anomalies above 90% significance level. MDR is shown by solid box. (b) Same as (a), but for wind stress (N m<sup>-2</sup>; vector). Red (blue) shading denotes weak (strong) anomalies above 90% significance.

## Figures

Fig.1

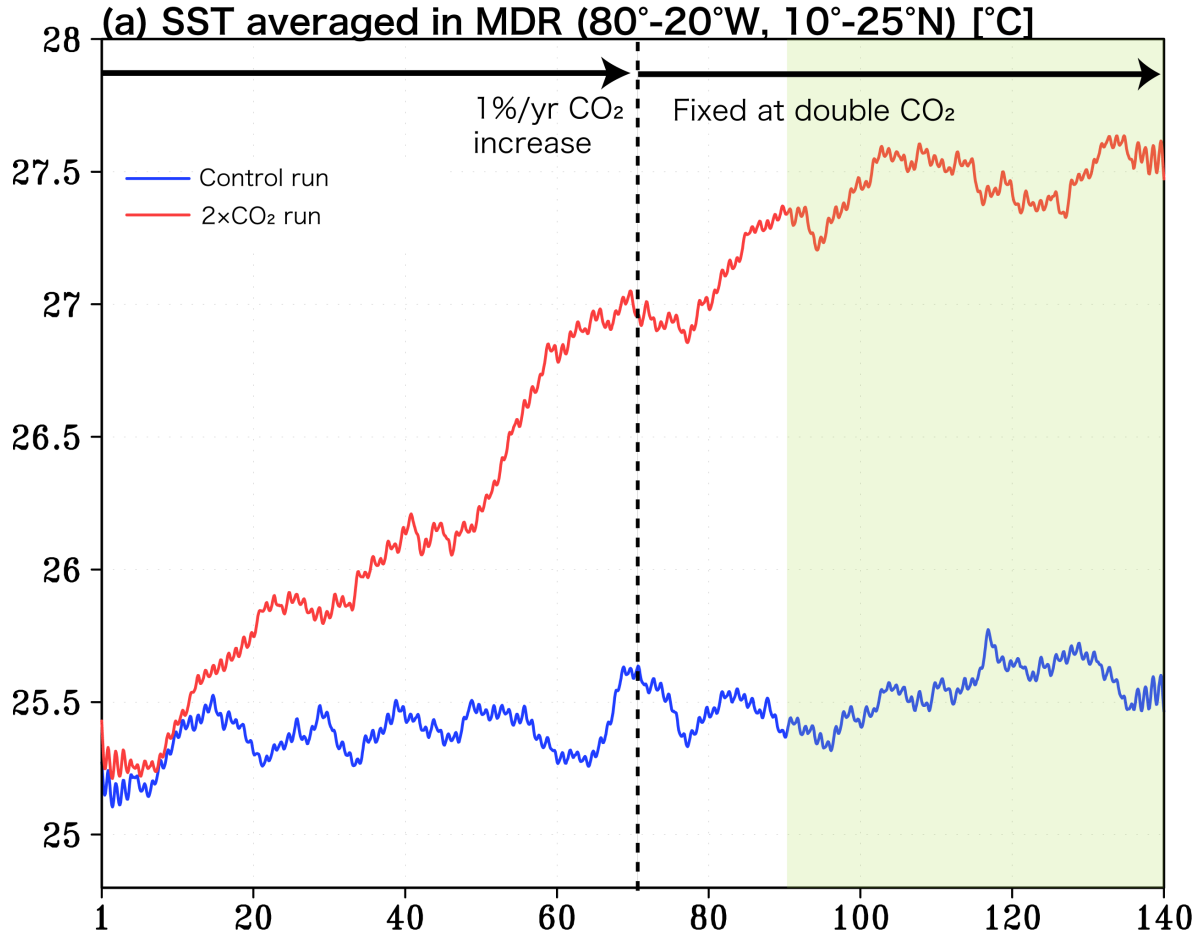
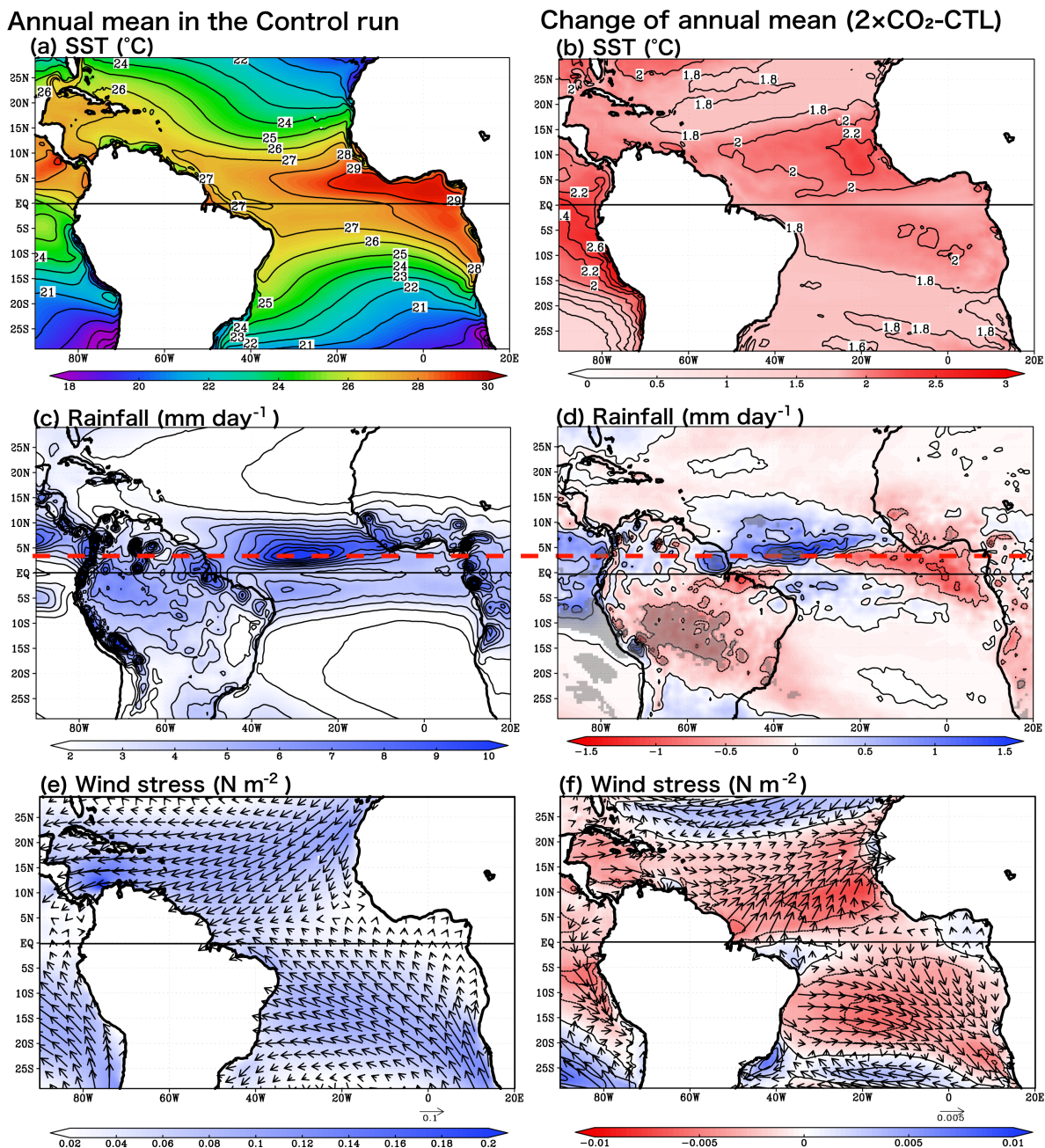


Fig. 1: (a) SST averaged in the Main Developing Region for Atlantic Hurricane (MDR: 80°-20°W, 10°-25°N) from the present-day Control run (blue line) and its CO<sub>2</sub> doubling run (red line) with CM2.5 in model years 1-140 (°C). This paper focuses on model years 91-140. A running mean of eight years is applied.

1 Fig.2



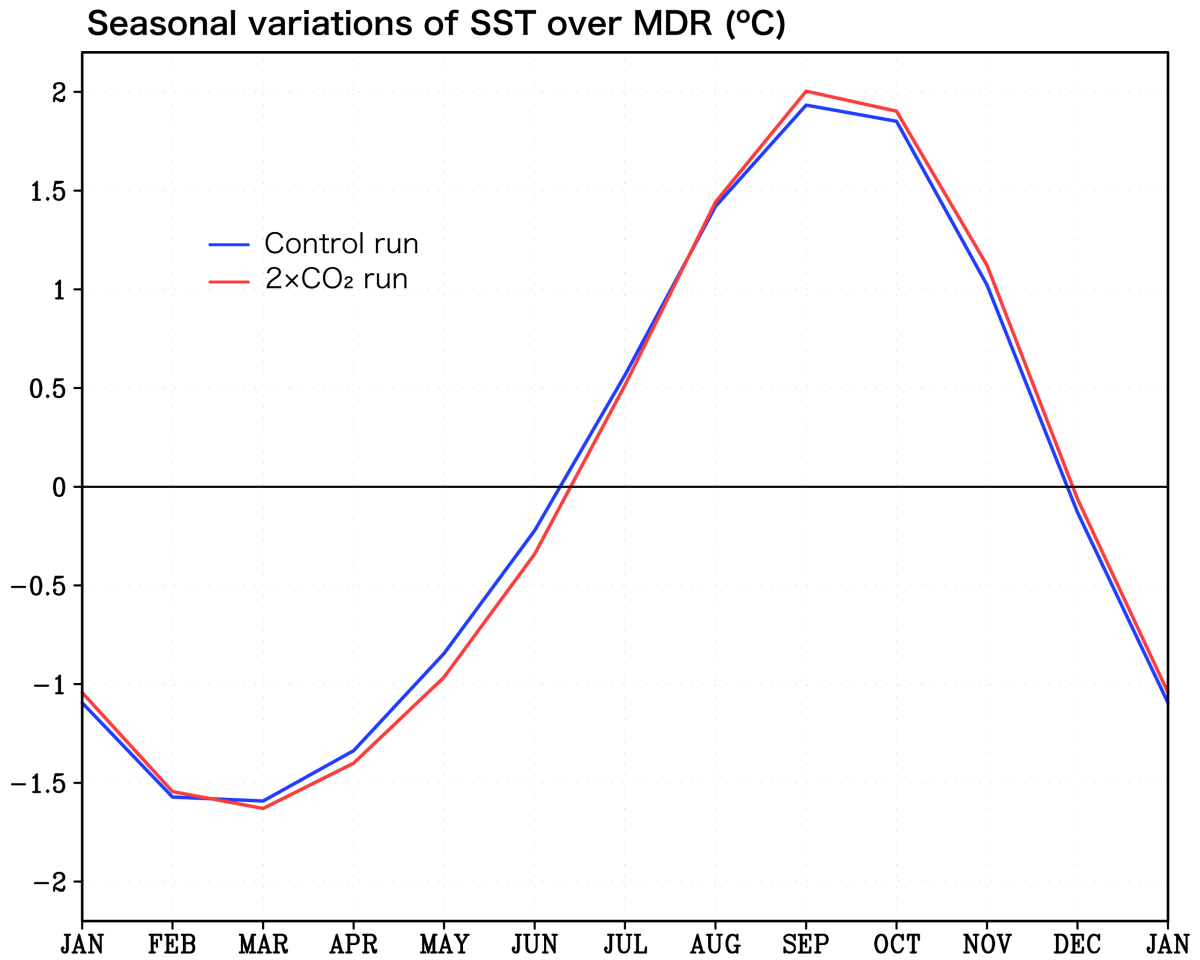
2

3 Fig. 2: (a) Annual mean SST in the Control run averaged in model years 91-140 (°C). (b)  
 4 Response to CO<sub>2</sub> doubling of annual mean SST (CO<sub>2</sub> doubling run minus Control run) in  
 5 model years 91-140 (°C). Note that the change in annual mean SST between CO<sub>2</sub> doubling  
 6 run and Control run is beyond one standard deviation of interannual variations of annual



1 mean SST in the Control run everywhere in this figure. (c) Same as (a), but for rainfall (mm  
2 day<sup>-1</sup>). Contour interval is 1mm day<sup>-1</sup>. Red dashed line shows the latitude of the mean  
3 Atlantic ITCZ in the Control run. Grey shading denotes that the change in annual mean  
4 rainfall between CO<sub>2</sub> doubling run and Control run is beyond one standard deviation of  
5 interannual variations of annual mean rainfall in the Control run. (d) Same as (b), but for  
6 rainfall. Contour interval is 0.5mm day<sup>-1</sup>. (e) Same as (a), but for wind stress (N m<sup>-2</sup>). (f)  
7 Same as (b), but for wind stress (N m<sup>-2</sup>). Contour interval is 0.0025N m<sup>-2</sup>.

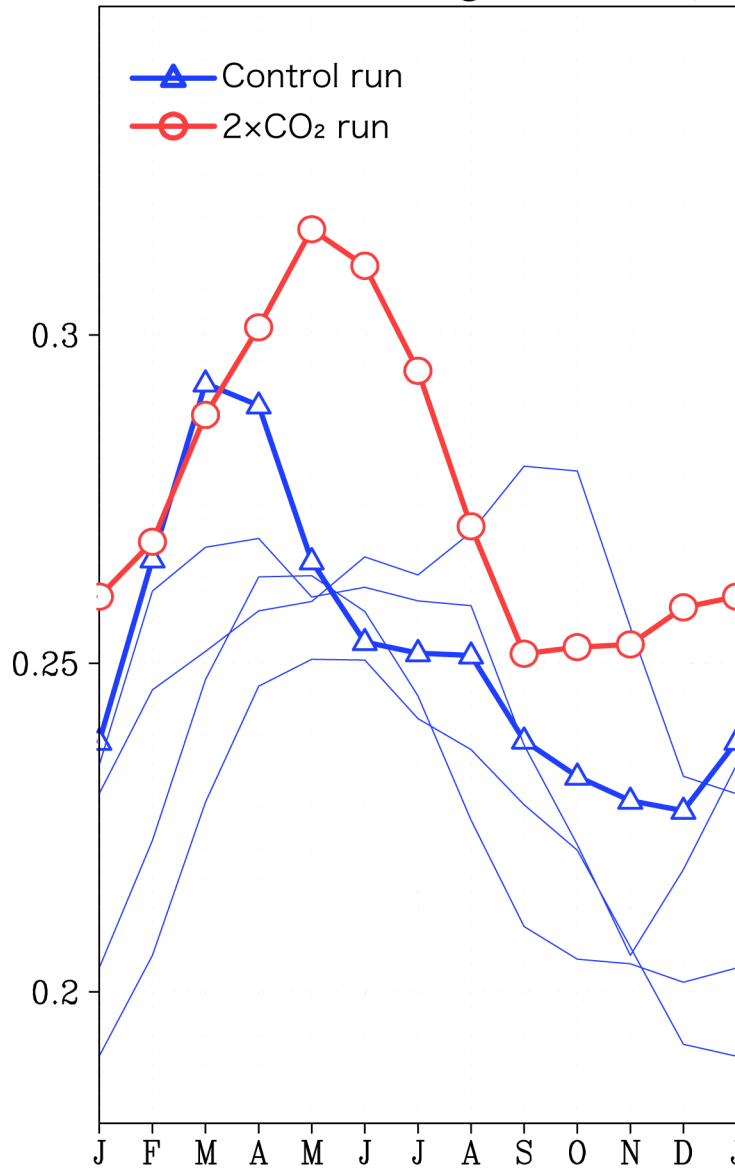
1 Fig. 3



2  
3 Fig. 3: Mean seasonal variations of SST<sub>MDR</sub> from the annual mean in the present-day  
4 Control (blue line) and the CO<sub>2</sub> doubling run (red line) (°C).

1 Fig. 4

(a) Standard deviation of interannual variations of SST averaged in MDR ( $^{\circ}\text{C}$ )

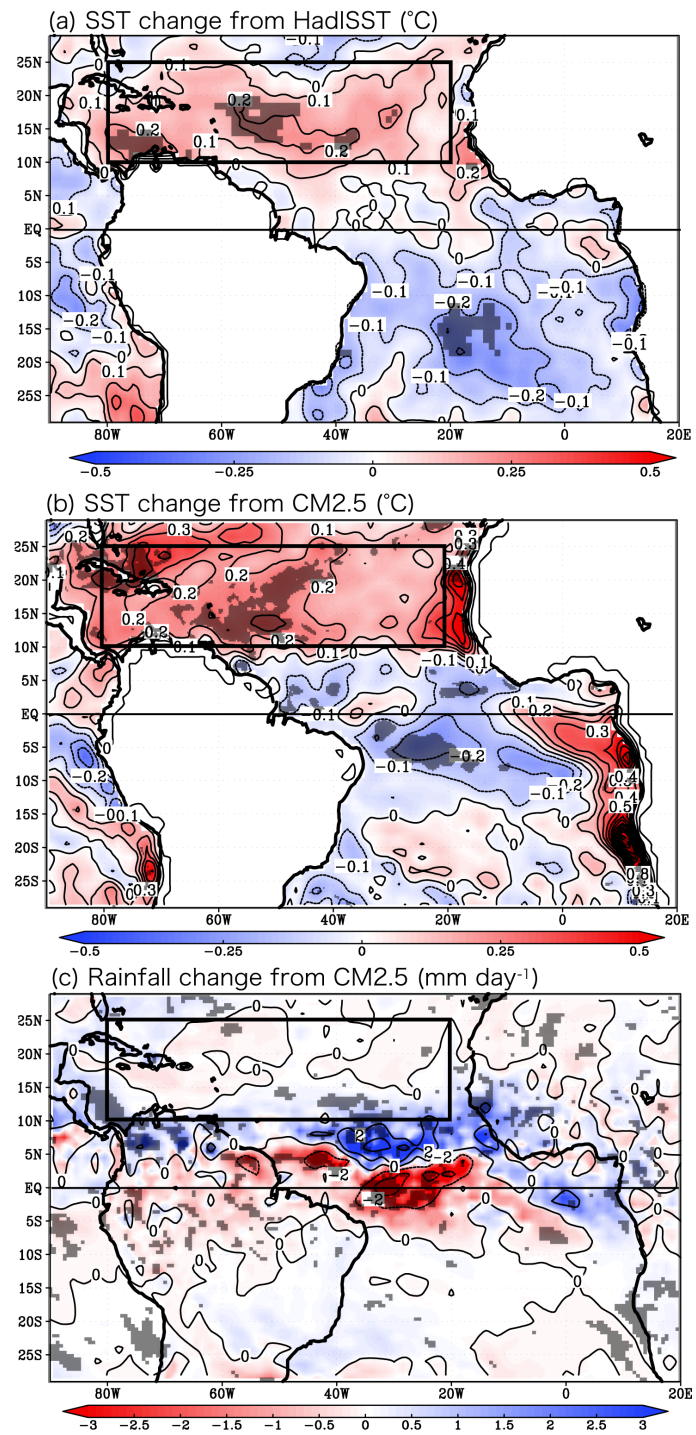


2

3 Fig. 4: (a) Monthly standard deviation of the interannual variation of the SST<sub>MDR</sub> for the  
4 present-day Control (thick blue line) and the CO<sub>2</sub> doubling run (thick red line) in model  
5 years 91-140 ( $^{\circ}\text{C}$ ). The thin blue lines show the four other 50-years mean standard  
6 deviations in the Control run. A running mean of three months is applied.

1 Fig.5

# Change in composite anomalies in MJJ of warm MDR years

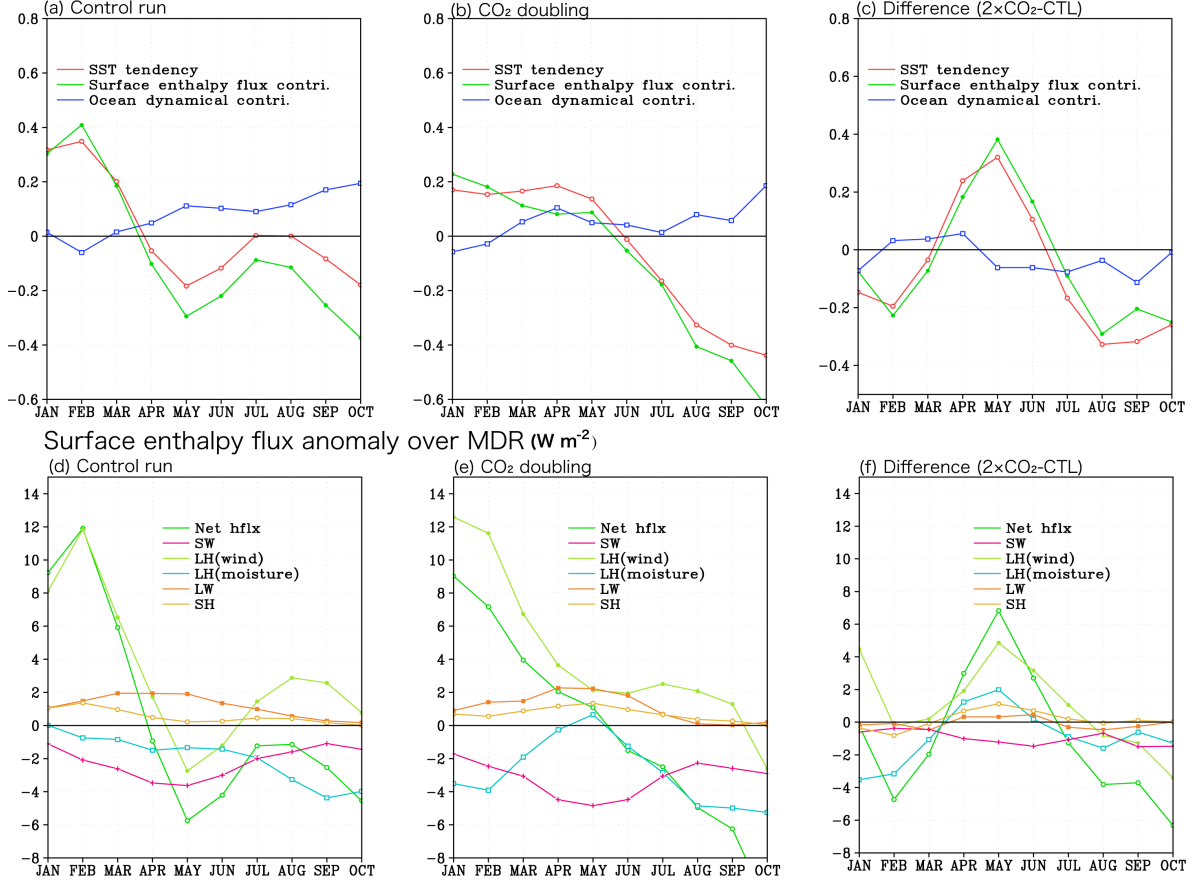


1 Fig.5: (a) Difference in composite anomalies for SST between the recent 50 years (1960-  
2 2009) minus the early 50 years (1881-1930) from the HadISST data for May-July in warm  
3 SST<sub>MDR</sub> years (°C). Contour interval is 0.1°C. Grey shading denotes anomalies above 90%  
4 significance level. MDR is shown by solid box. (b) Similar to (a), but response to CO<sub>2</sub>  
5 doubling of composite anomalies for SST in the CO<sub>2</sub> doubling run minus the Control run.  
6 (c) Same as (b), but for rainfall in the CO<sub>2</sub> doubling run minus the Control run (mm day<sup>-1</sup>).  
7 Contour interval is 1mm day<sup>-1</sup>.

1 Fig.6

### Warm MDR years composite

Mixed-layer heat budget anomaly over MDR ( $10^{-7} \text{ K s}^{-1}$ )



3 Fig. 6: Diagnostic bulk mixed-layer heat balance anomaly over the MDR ( $10^{-7} \text{ K s}^{-1}$ ). Rate

4 of change of  $\text{SST}_{\text{MDR}}$  is determined by  $\frac{Q - q_{\text{sw}}}{\rho C_p H_{\text{mix}}}$ : sea surface enthalpy flux contribution and

5 ocean dynamical contribution by Eq. (1) in the text. A running mean of three months is

6 applied. (a) Warm  $\text{SST}_{\text{MDR}}$  years composite in the Control run of CM2.5. (b) Same as (a),

7 but for the  $\text{CO}_2$  doubling run. (c) Same as (a), but for difference between the  $\text{CO}_2$  doubling

8 run and the Control run. (d) Warm  $\text{SST}_{\text{MDR}}$  years composite in the Control run for surface

9 enthalpy flux anomaly over the MDR ( $\text{W m}^{-2}$ ).  $Q$ : net surface enthalpy flux anomaly “Net.

10 Hflx” is determined by shortwave radiation “SW”, wind-induced latent heat “LH(wind)”,

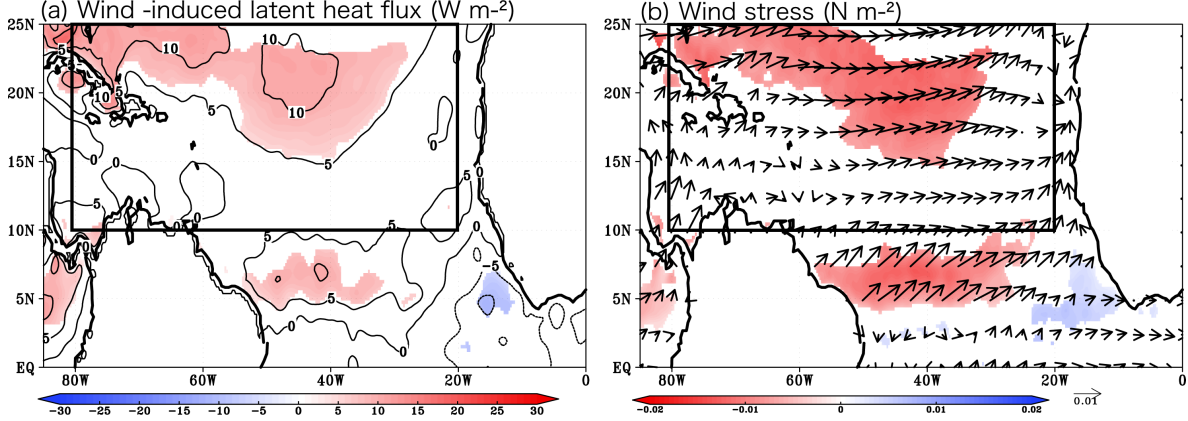
11 moisture-induced latent heat “LH(moisture)”, longwave radiation “LW”, and sensible

12 heat “SH” fluxes. A running mean of three months is applied. (e) Same as (d), but for the

- 1 CO<sub>2</sub> doubling run. (f) Same as (d), but for difference between the CO<sub>2</sub> doubling run and the
- 2 Control run.

1 Fig.7

**Difference in composite anomalies for AMJ in warm MDR years  
(2×CO<sub>2</sub>-CTL)**



2

3 Fig. 7: (a) Response to CO<sub>2</sub> doubling of composite anomalies for the wind-induced latent

4 heat flux in the CO<sub>2</sub> doubling run minus the Control run,  $\left. \frac{\partial Q_{LH}}{\partial W} \right|_{CO_2} W'_{CO_2} - \left. \frac{\partial Q_{LH}}{\partial W} \right|_{CTL} W'_{CTL}$  in

5 the text, for April-June in warm SST<sub>MDR</sub> years (W m<sup>-2</sup>). Positive values shows warming

6 ocean. Contour interval is 5W m<sup>-2</sup>. Color shading denotes anomalies above 90%

7 significance level. MDR is shown by solid box. (b) Same as (a), but for wind stress (N m<sup>-2</sup>;

8 vector). Red (blue) shading denotes weak (strong) anomalies above 90% significance.